Aalto-yliopisto
Aalto-universitetet
Aalto University

Master’s Programme in Automation and Electrical Engineering

Implementation of Reference Feedforward Power Synchronization Control in a Simulation Environment

Mohammad Osama Nasir Iqbal

Master’s thesis
2025

Aalto-yliopisto
Aalto-universitetet
Aalto University

Author Mohammad Osama Nasir Iqbal

Title of thesis Implementation of Reference Feedforward Power Synchronization Control in a Simulation Environment

Programme Automation and Electrical Engineering

Major Control, Robotics, and Autonomous Systems

Thesis supervisor Prof. Marko Hinkkanen

Date 19.11.2025 **Number of pages** 40 **Language** English

Abstract

This thesis presents the implementation and validation of the Reference-feedforward power synchronization control (RFPSC) method in a simulation environment. The RFPSC extends the classical power synchronization control (PSC) approach by introducing a feedforward term of the active-power reference, enabling enhanced damping and near pole-zero cancellation in the closed-loop response. A block-based simulation environment provides a graphical representation of the model and allows for component-wise tuning and testing. The implementation is evaluated under steady-state conditions, active-power steps under varying short-circuit ratios, and frequency deviations. The simulations demonstrate correct inherent synchronization, well-damped and effective active-power tracking and robust behaviour across varying grid strengths. The frequency deviation test further verifies the expected power-frequency coupling characteristics of PSC-based methods.

Keywords Grid-following converters, grid-forming converters, power synchronization control, reference-feedforward, stability, synchronization.

Table of contents

Acknowledgements

As I complete my master's thesis, I wish to express my gratitude for the support and guidance I have received throughout this journey. I begin in the name of Allah, the Most Gracious, the Most Merciful, and thank Him first and foremost. I also honour my late parents for the love and care with which they raised me.

I extend my gratitude to the management of Aalto University for providing an excellent environment for students, particularly the services offered by the *Starting Point of Wellbeing* department, from which I benefited often and deeply. My heartfelt thanks go to my academic mentor, Professor Ville Kyrki, and to the planning officer Alli Palojärvi, both of whom guided me through the journey of this master's degree and consistently pointed me in the right direction. This brings me to my thesis supervisor, Professor Marko Hinkkanen, who encouraged me to explore the world of grid-connected converters and electrification, and who supported this thesis with patience, kindness, and continued guidance. I offer him my sincere gratitude. I am also grateful for the brilliant colleagues and friends I met over these 2.5 years, with whom I shared ideas, laughter, and frustrations, creating cherished memories.

I would also like to thank my employer, SpectroCor Oy, for generously allowing me the flexibility in my work schedule to make out the time needed for this thesis. I then thank all those whose support, prayers, and presence shaped this journey, and particularly my family, and my sister's amazing kids, for remembering me in their prayers. And last, but not the least, I thank my amazing wife, Arshia, whose life was most impacted by the countless hours poured into this thesis, and supported me through it with patience and faith. May Allah reward all of you abundantly.

Abbreviations and Lists

Abbreviations

RoCoF	Rate of change of frequency
GFL	Grid following converters
PLL	Phase-locked loop
GFM	Grid forming converters
SM	Synchronous machine
VSM	Virtual synchronous machine
PSC	Power synchronization control
RES	Renewable energy sources
ENTSO-E	European network of transmission system operators for electricity
SCR	Short-circuit ratio
LPF	Low-pass filter
VSC	Voltage source converter
HVDC	High voltage direct current
PWM	Pulse-width modulation
RFPSC	Reference-feedforward power synchronization control
DC	Direct current
GW	Gigawatt
HIL	Hardware-in-the-loop
PCC	Point of common coupling

1. Introduction

Modern civilization is built on a stable and secure supply of electrical power. From hospitals to telecommunication systems and data centers, many essential activities depend on reliable and uninterrupted power. Traditionally, these power systems relied on large synchronous generators that generate electricity and provide support for stability. The rotating masses of these machines store kinetic energy which provides a cushion against abrupt mismatches between demand and generation. This buffer effect is known as the system's inertia and slows down the frequency deviations, thus buying time for control mechanisms to respond [1].

Over the decades, this stable framework has been reshaped by the shift toward low-carbon energy generation. Conventional centralized fossil-fuel power plants are increasingly being replaced by renewable and distributed generation technologies, such as photovoltaic systems, wind turbines, and battery energy storage systems. These sources interface with the grid through power-electronic converters instead of through rotating mass. As a result, they contribute no additional inertia to the grid [2], making it challenging to maintain frequency during sudden load or generation changes. It further increases the rate of change of frequency (RoCoF), threatening the reliability of protection schemes and reserve control mechanisms [3].

Grid-following converters (GFL) synchronize with the grid through phase locked loop (PLL), and hence have a risk of instability in weak grid conditions. As the penetration of renewable energy continues to grow, such weak grid scenarios become more challenging, leading to degraded performance and oscillatory behaviour [4]. In response to these challenges, growing attention is directed toward the development of Grid-Forming (GFM) converters that support the grid by emulating the behaviour of synchronous machines (SMs) [6], making them a key technology in enabling converter-dominated power systems for the future.

Over the years, numerous GFM control strategies have been proposed and developed to emulate the stabilizing characteristics of synchronous machines. Among them are Droop Control, Virtual Synchronous Machine (VSM), and Power Synchronization Control (PSC) [7], [9], [19].

PSC's design eliminates the need for PLL by achieving synchronization through active power control. The converter's internal frequency varies with the power error, and its voltage reference is generated by integrating this frequency, ensuring a natural synchronization with the grid through control logic [19], [20]. Since the control bandwidth and the dynamic characteristics of PSC are strongly influenced by the controller tuning and voltage magnitude [21], [22], the study in [23] addresses this gap by presenting a robust analytic design for PSC. It introduces explicit equations that relate the control gains to key system parameters, ensuring predictable behaviour in varying grid conditions. The study in [28] further enhances this robust analytic design for PSC by introducing a feedforward term of the active-power reference, which improves damping, and enables near pole-zero cancellation in the close-loop response.

This thesis presents a time-domain implementation and evaluation of this enhancement in a simulation environment. The model follows the formulation in [28], and its performance is evaluated under the active-power steps, varying grid strengths, and frequency deviations. The simulations are used to verify the expected synchronization, damping characteristics, and power-frequency coupling properties associated with PSC-based GFM methods.

The remainder of the thesis is structured as follows. Chapter 2 reviews the evolution of GFMs and the main control techniques with a dedicated sub-section on PSC. Chapter 3 describes the MATLAB/Simulink implementation and parameter derivation. Chapter 4 discusses the simulation results. Chapter 5 concludes with key findings, limitations, and recommendations for future research.

2. Literature Review

2.1 Power System Evolution and Motivation

Conventionally electric power has been generated by burning fossil fuels to drive large synchronous machines. However, due to a finite availability of these resources, and associated environmental concerns like greenhouse gas emissions, there has been a notable transition towards renewable energy sources (RESs) in the past couple of decades. This transition has reshaped the system at its core by motivating the adoption of converter-based power generation. These converter-based RESs connect to the grid through power electronics, which results in a lack of natural inertia contribution from the generators, and reduces the system's ability to resist sudden frequency deviations [29]. Figure 1 from the ENTSO-E report on inertia and RoCoF simulates the results of a 3 GW generation outage scenario for 2020 and 2030. It can be seen that the reduced share of SM-based generation leads to faster (higher RoCoF) and larger (deeper nadirs) frequency deviations, thus challenging the conventional protection and reserve mechanisms [2].

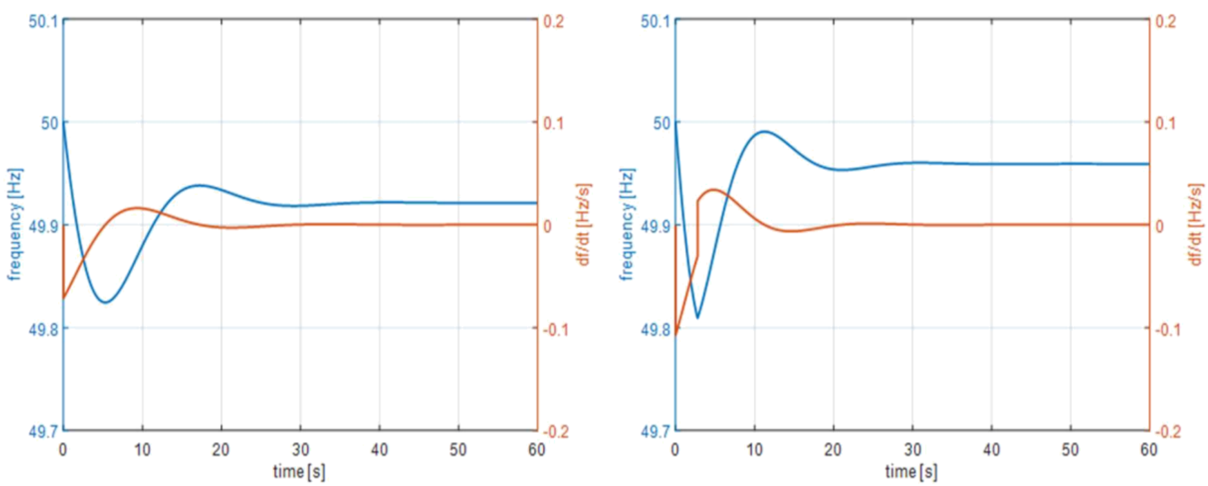

Figure 1: Frequency response following a 3 GW outage in the ENTSO-E system for the years 2020 (left) and 2030 (right) (adapted from [2]).

According to a survey of global revisions to the grid codes [3], several countries have updated their frequency response and synthetic inertia requirements, following a number of high RoCoF events, inadequate reserve capacities, and protection failures, in low-inertia power systems [3]. Furthermore, as the converters used in the RESs are predominantly GFLs [5], that synchronize with the grid voltage through PLL, they are prone to cause system instability, particularly in weak-grid conditions. These weak-grid conditions typically include high short-circuit impedance, in addition to the low-inertia [4].

Simulation-based study [6] shows that purely GFL converters have a higher risk of oscillations in the system as compared to hybrid systems, where some converters operate in GFM mode, thus improving the stability of the system [6]. Study [5] extends this analysis, showing that synchronous condensers and grid-forming energy storage systems enhance the stability margins of the renewable plants by improving their equivalent impedance, whereas static compensators, when lacking stored energy or rotating parts, offer limited support and still carry the risk of oscillations [5].

Table 1 compares the operational properties of traditional synchronous machines with modern converter-based generators. It can be seen that while the speed and responsiveness of modern generators are unmatched, they inherently lack inertia, synchronization, and frequency stability, which is the system's ability to maintain a steady frequency after an abrupt imbalance between load and generation [13].

Table 1. Comparison between synchronous machines and converter-based-generators.

Property	**Synchronous Machine**	**Converter-based Generators**
Inertia	Natural (mechanical)	None (unless emulated)
Synchronization	Rotor angle-based	PLL or GFM-based
Frequency stability	Inherent	Control-dependent
Fault response	Inherent current-limiting and overload tolerance	Software-controlled current-limiting
Control timescale	Mechanical (slow)	Electronic (fast)

Together, these discussions highlight a paradigm shift in electric power systems, from a mechanically driven, inherently inertia rich grid, to electronically dominated, fast-responding network, but one, in which stability must be actively maintained through control. This transition has encouraged the development of GFM converter control techniques, aimed at reproducing within the converter-based generation, the key characteristics of the SMs discussed above. The following subsection will discuss how the GFLs and GFMs shape the behaviour of modern renewable power systems.

2.2 Grid-Following (GFL) vs Grid-Forming (GFM) Converters

The highlighted need in the previous section for improved converter control strategies has led to the development of two distinct operational modes; Grid-Following and Grid-Forming. While both types are converter-based generation technologies, they differ fundamentally in their interaction with the power system, and hence their contribution to the grid.

Figure 2 shows a simplified representation of the commonly adopted classification that divides the grid-connected power converters into four main categories, grid-feeding, grid-forming, and two variants of grid-supporting control [7]. Grid-feeding converters are designed to operate as controlled current sources that must remain synchronized with the stiff grid voltage, using PLL synchronization. This behaviour is commonly referred to as grid-following control. Grid-supporting converters adjust their output according to droop characteristics, behaving either as current or voltage sources that can provide limited ancillary services but still rely on an external grid reference. On the other hand, grid-forming converters act as controlled voltage sources, capable of establishing voltage references and frequencies of their own, thus making them suitable for operation in weak or islanded systems [7]. Though the four categories were briefly discussed, the modern-day low-inertia systems largely depend on GFL and GFM converters.

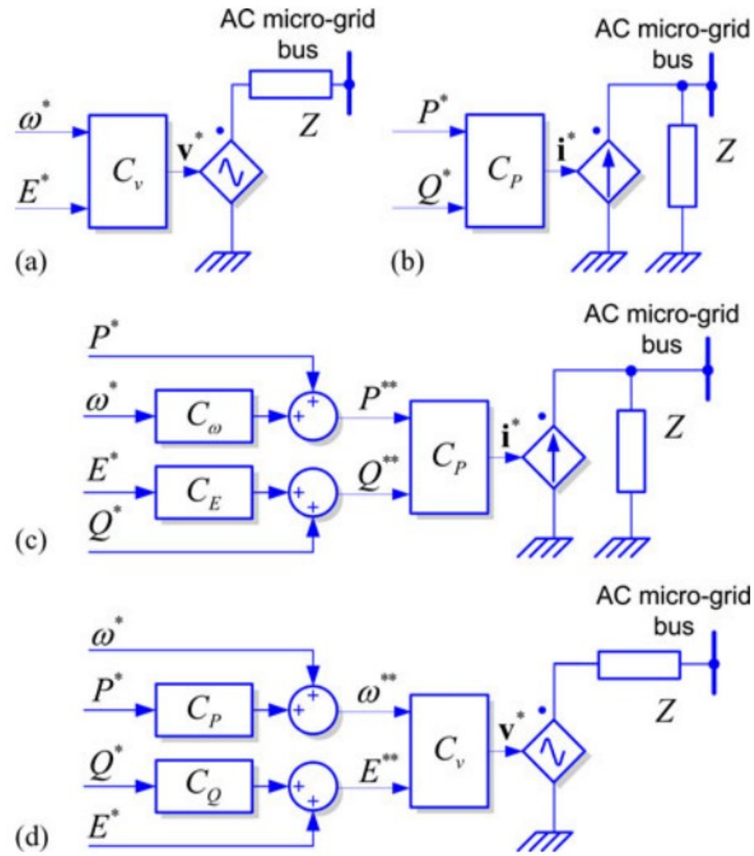

Figure 2. (a) grid-forming, (b) grid-feeding, (c) current-source-based grid-supporting, and (d) voltage-source-based grid-supporting (adapted from [7]).

2.2.1 Grid-Following Converters

GFL converters synchronize with the grid voltage with the help of PLL, regulating their output current accordingly. This technique introduces a heavy reliance on a strong grid with sufficient stiffness for stable operation, which means, the grid's impedance is low enough to maintain stable synchronization. But GFLs struggle when integrated with weak grids with low short-circuit ratios (SCRs); unmatched parameters between PLL and the grid impedances can lead to poorly damped oscillations and potentially, instability [4], [10]. These challenges raise questions about the potential scalability of GFL-based systems.

2.2.2 Grid-Forming Converters

GFMs address the key limitations of the GFLs by self-synchronizing to the grid without relying on an external phase reference, and can therefore demonstrate stable behaviour even in weak or islanded systems [8], [10]. While operating in synchronism with the grid, GFMs achieve this by directly regulating their output terminal voltage, and frequency dynamics, thus emulating the behaviour of SMs [8], [10]. Concepts such as synchronverters introduced the idea that inverters could replicate the swing dynamics of SMs by incorporating tunable inertia and other parameters such as friction coefficient and inductances [8]. Later work on the virtual synchronous machine (VSM) framework systematically classified the various control implementations, showing that VSM dynamics are mathematically linked to conventional droop-based control, particularly when the system operates under small-signal disturbances [9]. These research frameworks, and similar others collectively position GFMs as a versatile control technique, capable of both, frequency reference formation and inertia support, for modern power systems [10].

Although GFMs clearly offer significant advantages in system resilience and stability, some practical issues persist, such as the interoperability with conventional GFLs, current-limiting strategies, and large scale deployment [10]. Some proposals also include hybrid control strategies to reduce this gap between GFL and GFM operation. One example is the inertial PLL, which introduces inertia-like dynamics to regular PLL, thus merging the features of both the control techniques [11]. This indicates that the future converter systems may adopt a range of control capabilities, rather than sticking strictly with current classifications.

The growing importance of GFMs is not only evident in academic research, but has also started to reflect in emerging grid codes and technical standards. In 2024, ENTSO-E published its first interim report on *Grid-Forming Capability of Power Park Modules*, setting out initial technical requirements for GFM inverters within European networks [12]. These include capabilities such as:

- Establishing and maintaining internal voltage and frequency references
- Sustaining stable operation during grid disturbances
- Contributing to system frequency stability through synthetic inertia

The formal inclusion of such requirements into the grid codes marks a visible shift from mere theoretical development to practical implementation, qualifying GFMs as the preferred control paradigm for future grids. The following sections examine some principal control strategies developed for GFMs, while particularly focusing on power synchronization control (PSC).

2.3 Control Strategies for Grid-Forming Converters

The development of GFM converters has resulted in a wide range of control strategies, each characterized by distinctive philosophies, objectives, and implications for stability. Amongst the more widely discussed families are, droop-based control, VSM control, observer-based control, and PSC (which will be discussed in detail in the next sub-section). These approaches differ not only in their structure, but also in terms of their approach in addressing the most crucial challenges in the converter-dominated grids, discussed previously. As SM capacity continues to be replaced by power electronics, the capability to provide grid supporting attributes such as inertia, synchronism, and voltage stability becomes increasingly crucial for maintaining grid stability [2].

2.3.1 Droop Control

Droop control is a well established technique for power sharing in converter-based systems. Its principle is rooted in the governing dynamics of synchronous machines, i.e. as the generator increases its active power output, its operating frequency drops slightly. This natural characteristic allows multiple generators (or converters that emulate them) to share load in proportion to their droop coefficients, without requiring fast communication [1], [7].

The active power-frequency relationship can be expressed as

$$\omega = \omega_1 - K_p\left(P - P_{ref}\right) \quad (1)$$

where ω is the converter's angular frequency, ω_1 is the nominal grid frequency, K_p is the droop gain, P is the measured active power, and P_{ref} is the reference power.

Although this control law provides steady-state power sharing, it inherently lacks inertia. As a result, any changes in power cause the frequency to react instantaneously. To mitigate this, low-pass filters (LPFs) are often incorporated into the power control loops [18]. The inertia emulation operates by injecting (or absorbing) power during frequency events, effectively exchanging energy between the converter and the grid, making the response constrained by the DC-link capacity [24]. Figure 3 shows a block diagram of a droop-controlled voltage source converter (VSC). It shows LPFs incorporated into the active and reactive power control loops.

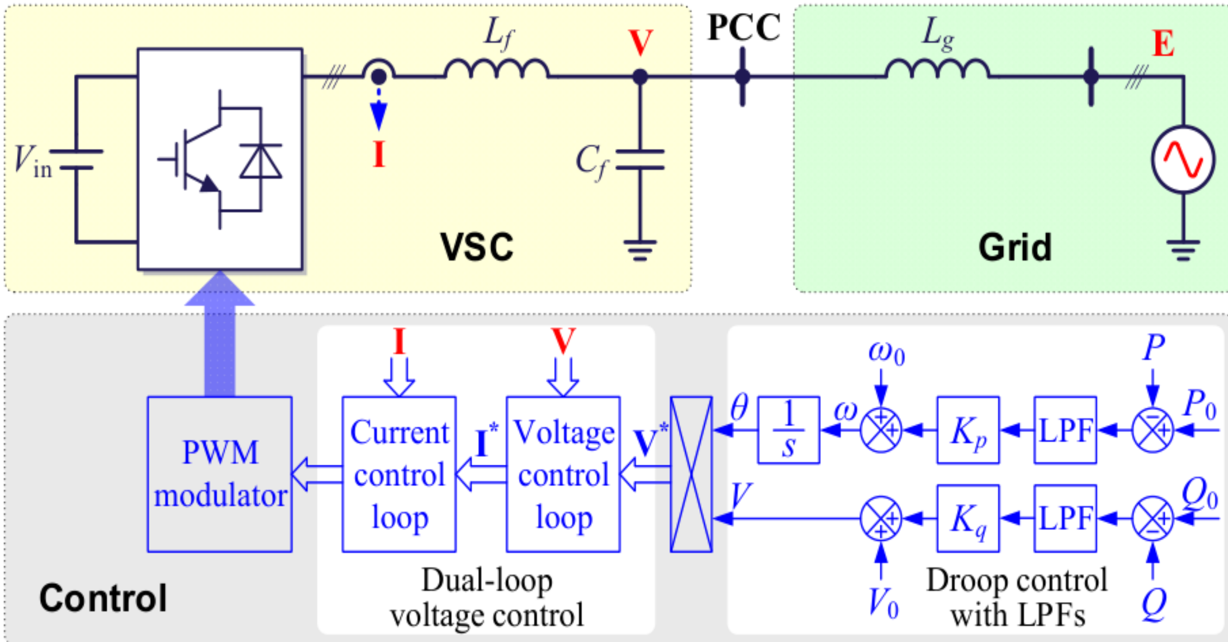

Figure 3. VSC with droop control and inertia emulation using LPFs, (adapted from [18]).

These filters slow down the dynamic response, mimicking the inertial behaviour of SMs, smoothening abrupt power deviations. However, the phase delays introduced by LPFs can adversely affect stability, and in case of poor tuning, may significantly reduce the system's stability margin [18].

2.3.2 Virtual Synchronous Machine (VSM) Control

While droop control captures the steady-state behaviour of SM, VSM control takes this further by explicitly incorporating the swing equation. As a result, unlike droop, VSMs introduce both inertia and damping dynamics, in addition to the static power-frequency response. The governing model is given by:

$$2H\frac{d\omega}{dt} = P_m - P_e - D(\omega - \omega_{nom}) \tag{2}$$

where H is the inertia constant, D is the damping factor, P_m is the mechanical input power, and P_e is the electrical output power [9]. Figure 4 illustrates the VSM control structure, where power–frequency droop is integrated with the swing equation to emulate both steady-state and dynamic behaviors of a synchronous machine.

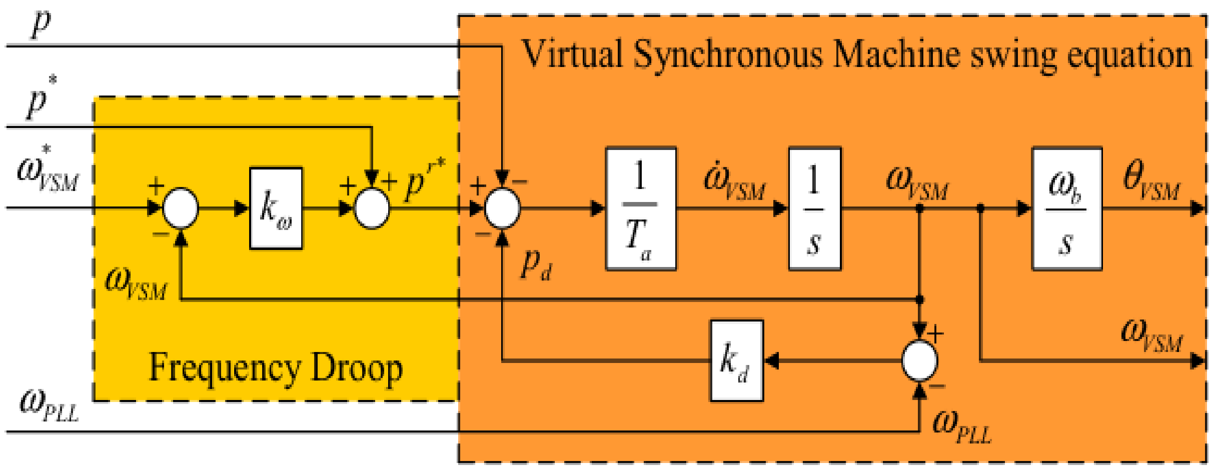

Figure 4. VSM structure combining power-frequency droop with swing equation (adapted from [14]).

By regulating frequency through the embedded swing equation (2), a converter can directly emulate the dynamic characteristics of synchronous machines, hence, maintaining synchronism and enhancing frequency support in weak-grid conditions [10]. However, this benefit comes with practical challenges. Firstly, the performance of VSMs is highly sensitive to parameter tuning, and poorly selected inertia or damping values can lead to oscillatory behavior [14].

A number of enhancements have been proposed to make VSMs more resilient in practice. As an example, study in [15] shows that integrating adaptive virtual impedance with a washout filter (a high-pass filter that allows transient inputs to pass, while rejecting steady-state and DC components), can improve the stability of parallel VSMs by enhancing coordination in power sharing, while preserving strong frequency support [15].

2.3.3 Observer-based Control

More recently, observer-based strategies have emerged as an alternative to both, droop and VSM approaches. Instead of emulating SM dynamics, these methods employ disturbance observers to estimate grid states and unknown inputs directly.

In their basic form, disturbance observers estimate the equivalent disturbance (representing the mismatch between generated and demanded power) acting on the system, and compensate for it by adjusting the controller output, thus achieving robust synchronization and disturbance rejection [16]. Building on this foundation, multifunctional observer-based controllers have been developed, that allow a converter to seamlessly switch between GFL and GFM modes without any structural modification [17]. Figure 5 presents the control structure of a disturbance-observer-based GFM converter. This light-weight design philosophy of the method achieves synchronization through estimation rather than emulating SM dynamics or relying on a PLL [17]. Whereas Table 2 compares the three GFM control strategies discussed in this subsection.

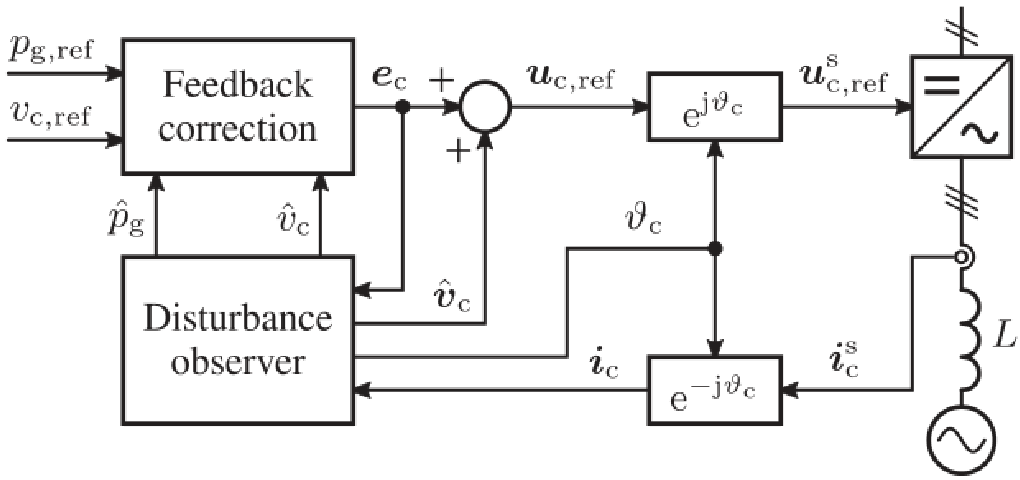

Figure 5. Disturbance observer-based grid-forming control structure, (adapted from [17]).

Table 2. Overview of Main GFM Control Strategies

Control Strategy	**Key Features**	**Advantages**	**Limitations**
Droop Control [18]	*Power-frequency droop with optional LPF-based inertia*	*Simple, decentralized*	*No real inertia*
VSM Control [9]	*Swing-equation-based inertia and damping emulation*	*Explicit inertia, stable frequency response*	*Parameter-sensitivity, computationally complex*
Observer-based Control [16], [17]	*Disturbance estimation replaces PLL and SM emulation*	*Robust, seamless mode switch*	*No inherent inertia*

Inertia, therefore, remains a central theme across grid-forming strategies and essentially defines the converter’s response to frequency deviations and power imbalances. These insights lead to the next section, which introduces PSC as a distinct approach. Unlike the three methods reviewed in this section, PSC achieves synchronization through active power feedback and can emulate inertia using a simple LPF.

2.4 Power Synchronization Control (PSC)

2.4.1 Fundamentals of Power-Synchronization Control

PSC has emerged as a distinct and effective GFM control approach which operates on the foundation that synchronization can be directly achieved through the relationship between converter output power, and the internal frequency [23]. PSC continuously regulates its frequency using instantaneous active-power feedback. This direct coupling allows PSC to naturally mimic the self-synchronizing behaviour of the SMs, without having to explicitly emulate mechanical inertia [19].

In its fundamental form, PSC defines the converter's angular frequency as a function of the Power error, given by eq (1). The control angle θ is obtained by integrating ω. Based on this angle, a voltage phasor of fixed magnitude is generated, forming a modulation reference for the converter. Through this mechanism, the converter achieves synchronization with the grid, purely through power feedback [19], [23]. This overall structure is shown in Figure 6, comprising the frequency control law, the phase-angle integrator, and the voltage-reference generation.

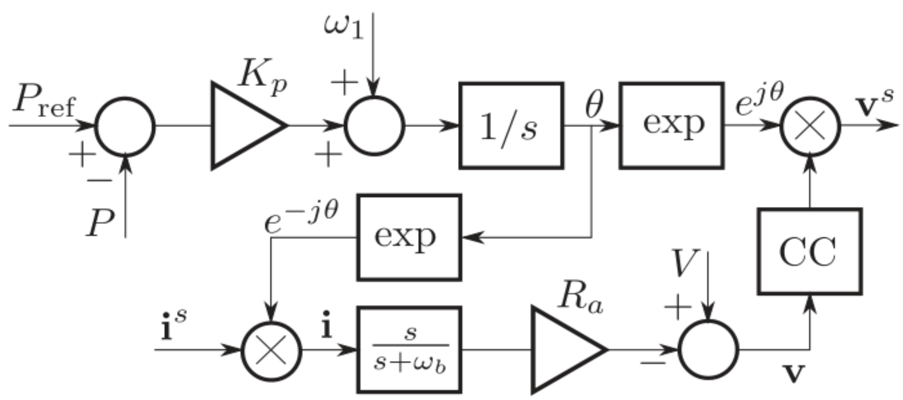

Figure 6. Block diagram of the classical PSC (adapted from [23]).

2.4.2 Stability Characteristics and Weak-Grid Performance

The study in [20] demonstrated that PSC can maintain synchronization even between two very weak grids linked by a VSC-HVDC link, a scenario in which conventional PLL-based current controllers fail. Further work in [21] analyzed the stability of PSC using a Jacobian transfer-matrix approach, which defines the input/output with the instantaneous value representation. This analysis revealed that PSC may experience instability beyond a specific power-transfer threshold, very much like the static-angle stability limit of SMs. These studies therefore established that PSC exhibits very similar stability characteristics as SM, strengthening it as a robust GFM solution for weak or islanded systems.

Later, study in [22] proposed a design-oriented transient-stability framework, that identified critical clearing angles, and showed that PSC possesses an inherent ability to restore synchronism after disturbances. The analysis revealed that PSC's transient performance is fundamentally influenced by the proportional gain K_p and the converter voltage magnitude. However, the value of K_p cannot be arbitrarily chosen and must be selected carefully.

2.4.3 Robust Analytic Design of PSC

Building on these developments, a comprehensive analytic design methodology was introduced in [23]. This robust design framework derives closed-form expressions for determining the proportional gain K_p, based on system parameters: grid frequency, base impedance, and converter voltage magnitude. The approach allows the controller to be scaled across different systems without requiring complex numerical tuning.

The analytical model of the active-power and dc-link control dynamics used for robust gain derivations is shown in Figure 7. This formulation incorporates the effects of grid impedance and converter-filter dynamics, ensuring stability over a wide range of grid strengths.

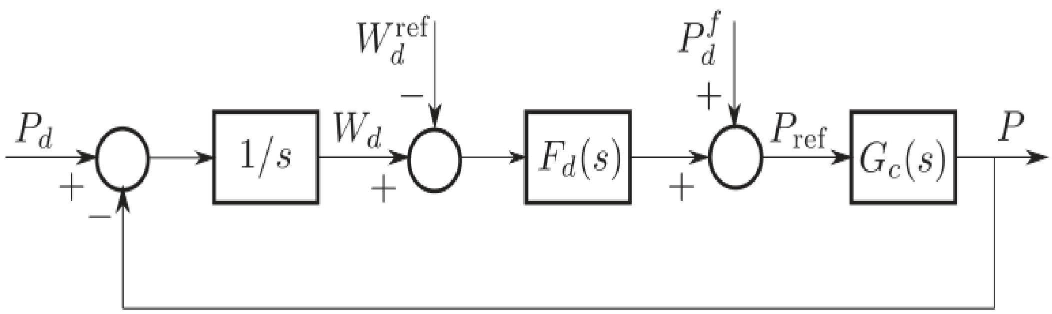

Figure 7. Analytical model of the active-power and dc-link control dynamics used for robust Kp gain derivation (adapted from [23]).

2.4.4 Inertia Extension and Dynamic Enhancement

A key extension to the robust analytic design is the emulation of virtual inertia, which can be implemented by adding an LPF to the PSC control law [23]. This filter introduces an inertial lag thus, mimicking the swing dynamics of SMs. The conceptual structure of this modification is shown in Figure 8, and illustrates how the filtered frequency feedback makes the control loop behave as if it had mechanical inertia [23].

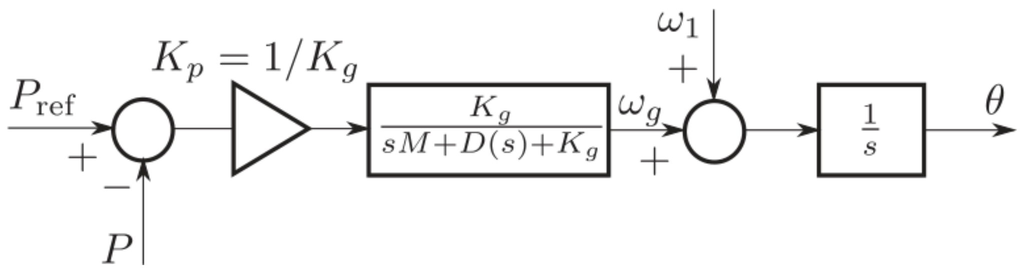

Figure 8. Extension of PSC with an LPF emulating virtual inertia and damping (adapted from [23]).

This robust analytical PSC framework offers multiple key advantages such as eliminating the need for iterative parameter tuning, and providing large enough stability margins. Furthermore, the design equations are expressed in system parameters rather than abstract gains, making the framework suitable for implementation and validation within simulation platforms.

2.4.5 Reference-feedforward PSC (RFPSC)

Study done in [28] extends the dynamic performance of the classical PSC and the robust analytical model presented in [23] by introducing a direct feedforward of the power reference signal into the voltage reference synthesis via the active resistance term. By aligning the feedforward and feedback terms, this method is able to achieve near-perfect pole-zero cancellation, effectively reducing the order of the system and simplifying its dynamics. Figure 9 illustrates the block diagram of the RFPSC enhancement of the classical PSC. The thick line shows the feedforward path for the reference active power.

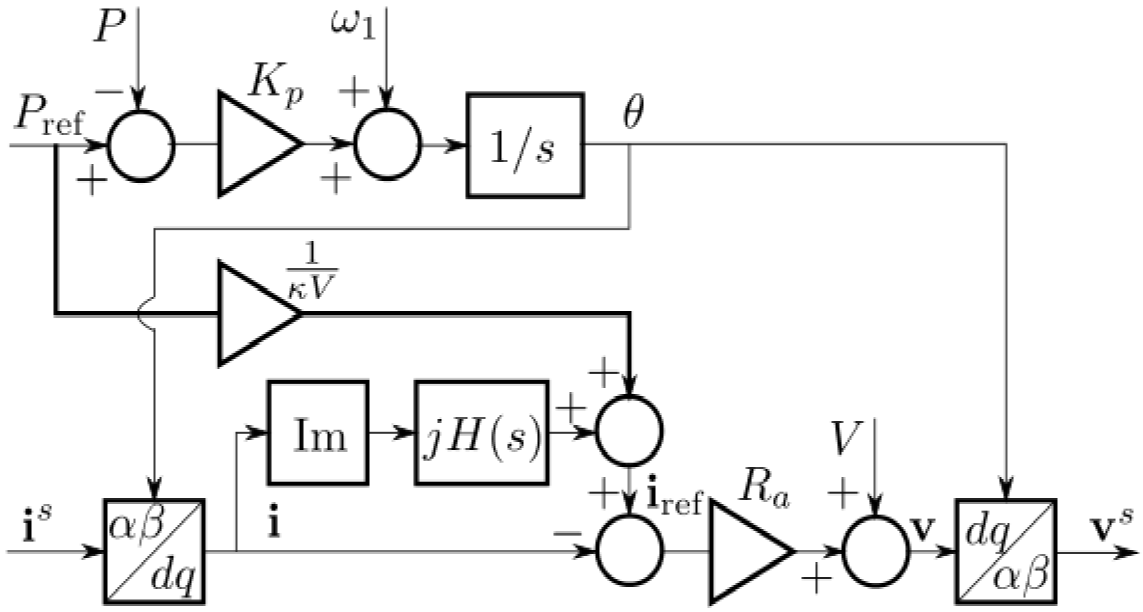

Figure 9. RFPSC block diagram (adapted from [28]).

This extension eliminates the step-response ringing and overshoot observed under strong-grid conditions operation of the classical PSC, while retaining the same robust gain selection criteria proposed in [23]. Furthermore, by transforming the closed-loop dynamics into an almost first-order response, RFPSC enables smoother and faster power tracking without compromising stability across grid strengths.

2.5 Simulation environment

Simulation environments provide a strong setting for studying power electronic converters and their control strategies. Environments with graphical and block-based architecture are particularly well-suited for analyzing the interaction between electrical dynamics, control algorithms, and measurement processes, enabling exploration of both steady-state and transient behaviour.

One commonly used example of such a simulation environment is Simulink, which is adopted for applications in converter studies. For example, the harmonic power-flow framework presented in [25] employs Simulink based time-domain validation to validate analytical predictions of converter models in polyphase grids. Similarly, the GFM converter study in [26] develops and validates multiple control strategies within MATLAB, providing a unified platform for assessing their performance under different grid strengths and disturbance scenarios.

Within this context, MATLAB provides a platform for implementation and validation of the RFPSC proposed in [28] and discussed in the previous subsection in detail. Implementing this enhanced framework in a simulation environment allows evaluation of its dynamic performance across a range of grid strengths, in a modular manner.

3. Methodology

3.1 RFPSC Simulink Implementation

As discussed in the previous section, this study aims to implement and validate the reference feedforward enhancement of the PSC method [28], using the MATLAB/Simulink environment. This implementation assesses the controller's steady-state and transient performances under realistic grid conditions.

Figure 10 illustrates the block diagram of the overview of the RFPSC model as implemented in Simulink. The control structure regulates the converter's internal frequency and voltage phase angle according to the PSC law [28]. The converter aligns its voltage phase angle with the grid by comparing the reference power P_{ref} and the calculated output power P, enabling synchronization without relying on PLL. The reference-feedforward stage adds a direct path from P_{ref}, thus shaping the converter's current reference for faster and better damped response. The active resistance and voltage synthesis block produces the converter's internal voltage which then interacts with the grid in the system model through the filter inductance. The resulting current, along with the synthesized voltage reference, computes the converter's instantaneous power P, which is then compared with reference power, thus closing the synchronization loop.

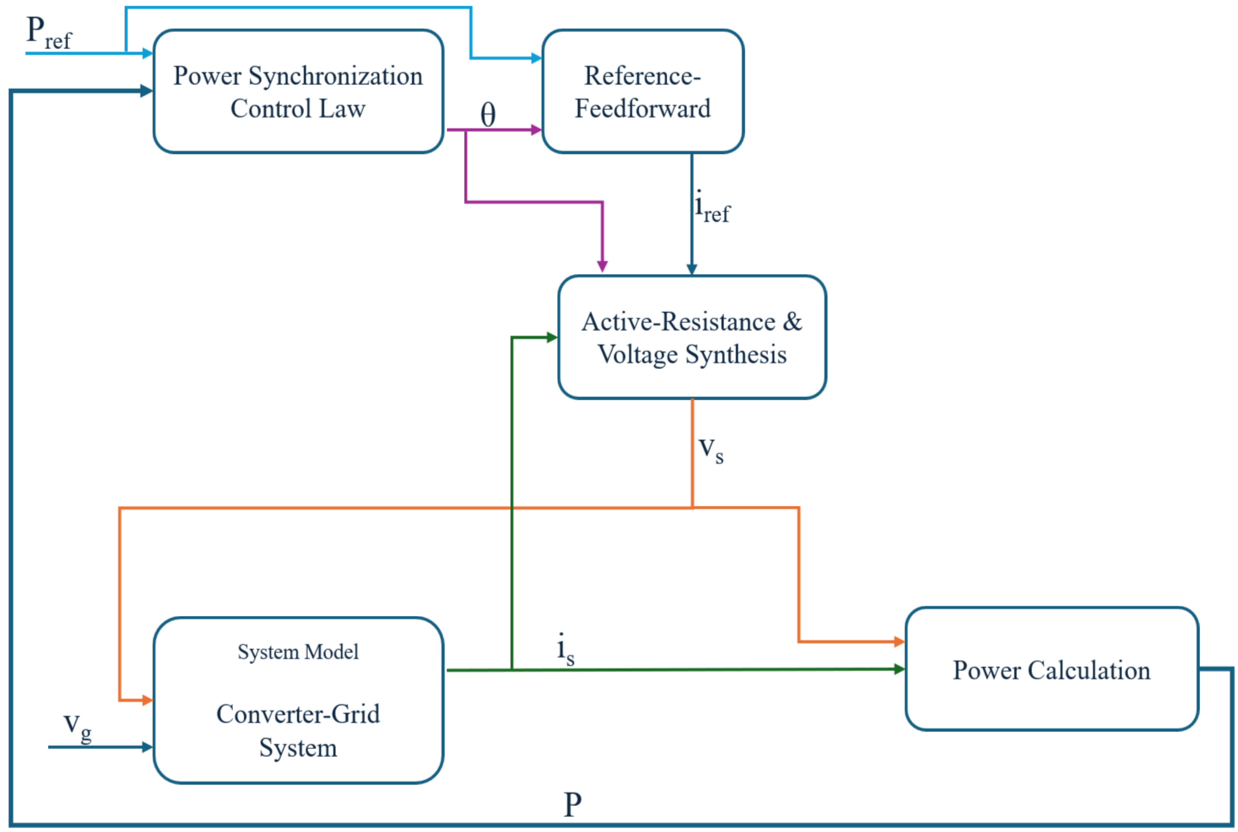

Figure 10. A block diagram of the overview of RFPSC model

where v_s is the converter-side voltage, $i_s$is the converter current, and i_{ref} is the reference current discussed in section 3.1.2. Each block in Figure 10 represents a subsystem within the overall model, and will be discussed in detail in the following sub-sections, along with their governing equations. This hierarchical structure of the RFPSC framework allows for modular testing and tuning. The controller gains and parameters follow the values used in [28] and shown in Table 3.

Table 3. System Parameters and Controller Gains.

Parameter	Actual Value	Normalized Value
Rated Power	12.67 kVA	1 p.u.
Rated Voltage	√(2/3) * 400 V	1 p.u.
Rated Current	√2 * 18.3	1 p.u.
Base Impedance	12.62	1 p.u.
Fundamental Frequency	50 Hz	1 p.u.
Active Resistance Ra	2.52 Ω	0.2 p.u.
Filter bandwidth Wb	31 rads/s	0.1 p.u.
Power-invariant constant κ	1.5	
Proportional gain Kp	0.005	

3.1.1 Power Control Law

The PSC law directly regulates the converter's internal frequency and voltage angle based on active-power feedback. Emulating the synchronization behaviour of a synchronous machine, its control law defines how the converter's frequency ω_c responds dynamically to the active-power error. This law is shown in eq (1). The instantaneous converter angle θ_c is obtained by integrating the frequency

$$\theta_c = \int \omega_c \, dt \qquad (3)$$

This approach allows the converter to synchronize with the grid through power exchange. If the converter delivers a smaller power than demanded ($P < P_{ref}$), the frequency increases, causing θ_c to increase, thus causing the converter's voltage phase to lead until power balance is achieved. Similarly, if $P > P_{ref}$, the phase lags, enabling the PSC to autonomously align the converter with the grid. The proportional gain is derived analytically as per [23], as

$$K_p = \frac{\omega_1 R_a}{\kappa V^2} \qquad (4)$$

where R_a is the active-resistance gain that provides damping. κ is the power-invariant scaling factor, and V is the converter's line-to-neutral peak reference voltage. Figure 11 shows the block diagram of the PSC law.

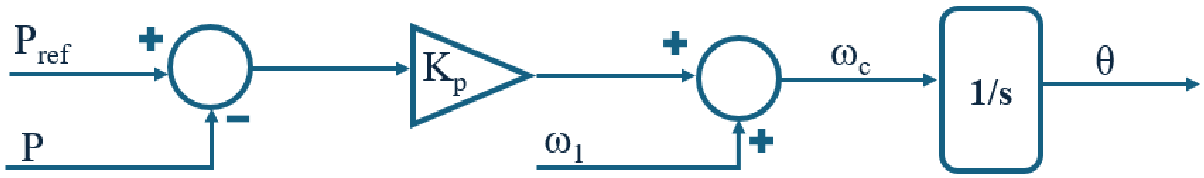

Figure 11. Block diagram of power control law

3.1.2 Reference-Feedforward

The reference-feedforward stage enhances the conventional PSC method by introducing the power reference into the current reference generation. The reference current is therefore defined as

$$i_{ref} = \frac{P_{ref}}{\kappa V} + j\, H(s)\, Im\,(i) \qquad (5)$$

where $H(s) = \frac{\omega_b}{s + \omega_b}$ is a low-pass filter applied to the q-axis current. The first term feeds forward the active-power reference while the second, filtered term preserves smooth dynamics. This feedforward method achieves near pole-zero cancellation in the closed loop, improving damping and transient response compared with conventional PSC [28]. Figure 12 shows the block diagram of the reference-feedforward implementation.

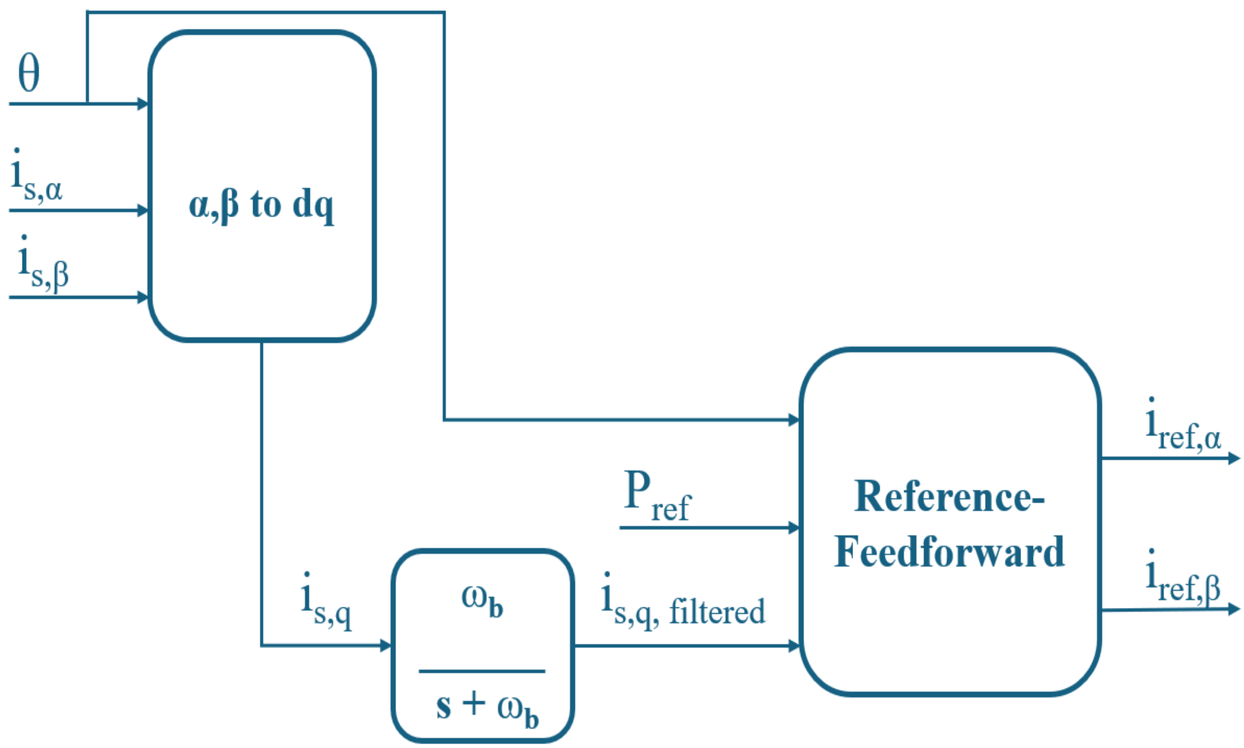

Figure 12. Reference-feedforward block diagram.

3.1.3 Active Resistance and Voltage Synthesis

While the power control law enables synchronization, it inherently lacks damping, and can lead to oscillations on its own. To improve the stability, an active-resistance term is introduced in the voltage synthesis, emulating a virtual resistive voltage drop. This term provides effective damping against transient power changes, without altering the core PSC principle. The resulting reference voltage is given by

$$v_s = V + R_a\left(i_{ref} - i_s\right) \qquad (6)$$

where the term $R_a\left(i_{ref} - i_s\right)$ acts as the damping component, and at steady state, when $i_{ref} \approx i_s$, it becomes negligible. The current references are fed in from the reference-feedforward block. Since the analysis in [28] assumes linear pulsewidth-modulation (PWM) operation with negligible latency and switching harmonics, the synthesized voltage is applied directly to the grid model.

3.1.4 Grid Model

The grid model represents the plant or the physical interface between the converter and a stiff grid, modeled as an infinite bus with constant voltage and frequency, connected through a purely inductive impedance. The system dynamics are expressed as

$$L\frac{di_s}{dt} = \left(v_s - v_g\right) \tag{7}$$

where L is the filter inductance. The grid voltage is generated as a balanced sinusoidal source with fixed amplitude V_g and grid voltage phase angle θ_g and is given by $v_g = V_g e^{j\theta_g}$. And θ_g evolves according to

$$\theta_g = \int \omega_g \, dt \tag{8}$$

where $\omega_g = \omega_1$ under nominal conditions. This simple grid model allows controlled frequency variation, allowing for evaluating synchronization under varying conditions. Figure 13 illustrates the system model as a block diagram.

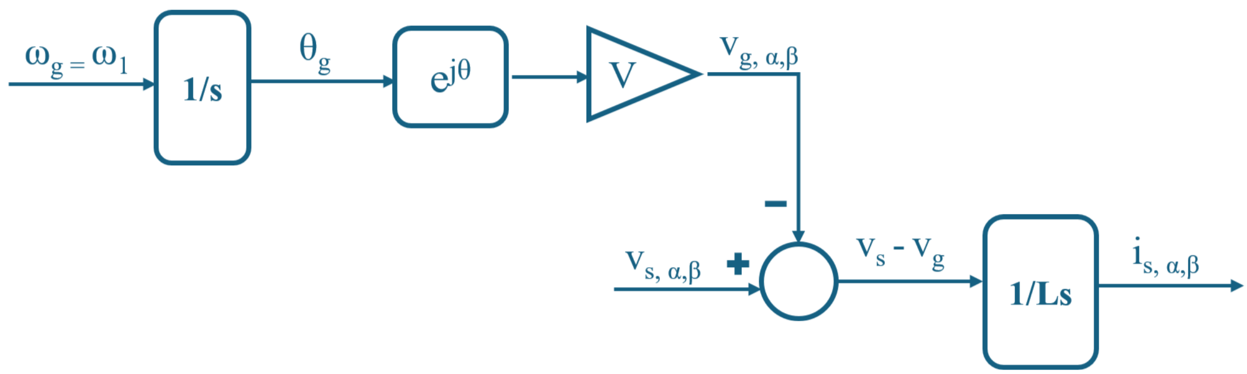

Figure 13. Block diagram for the grid model

3.1.5 Power Calculation

The instantaneous active power exchanged between the converter and the grid is calculated in the stationary α,β frame using the converter side voltages and currents as

$$P = \kappa\, Re\{ v_s\, i_s\, *\} = \kappa \left(v_{s,\alpha} i_{s,\alpha} + v_{s,\beta} i_{s,\beta}\right) \qquad (9)$$

This active power is fed back to the power control law block, where it is again compared with the reference power, thus closing the outer control loop.

3.2 Test Sequences for Validation

With the reference-feedforward power synchronization controller implemented in Simulink, a series of simulation tests is conducted to evaluate its performance and robustness. These tests replicate the validation scenarios reported in [23] and [28], covering steady-state and transient operating conditions.

The four tests are listed in Table 4. The corresponding validation goals, results, and analyses of these tests will be presented in Chapter 4.

Table 4. List of validation tests for the implemented model.

Test No.	Test
1	Active-power step up and down
2	Active-power step in varying grid conditions
3	Frequency Deviation

4. Performance Evaluation and Results

This chapter presents the simulation results of the implemented RFPSC model, evaluating its performance under steady-state and dynamic operating conditions.

4.1 Active-Power Step Response

In this test the reference power is subjected to a step sequence of P_{ref}= 0.2 p.u. + 0.3 p.u. + 0.5 p.u. - 0.75 p.u. The converter operates in moderate grid conditions (SCR = 4). Figure 14 (a) illustrates how the calculated active-power accurately tracks the varying reference in both cases, demonstrating the fast and stable regulation of the active-power. This well-damped response is consistent with the RFPSC model where the feedforward term cancels the zero introduced by the active resistance, producing an effectively first-order closed-loop behaviour. This characteristic is preserved across grid strengths, as discussed next. Figure 14 (b) shows the corresponding voltage magnitude during the step sequence. The voltage magnitude shows small transients at each active-power step due to the momentary change in the converter current. As expected, the voltage-magnitude deviations remain well controlled and settle quickly. Figure 14 (c) shows the currents d-axis and q-axis currents during these active-power steps. The d-axis current increases and decreases according to the power steps, and the transitions remain smooth and well-damped. While the q-axis current stays close to zero, with only minor disturbances, indicating stable current behaviour under balanced-grid conditions.

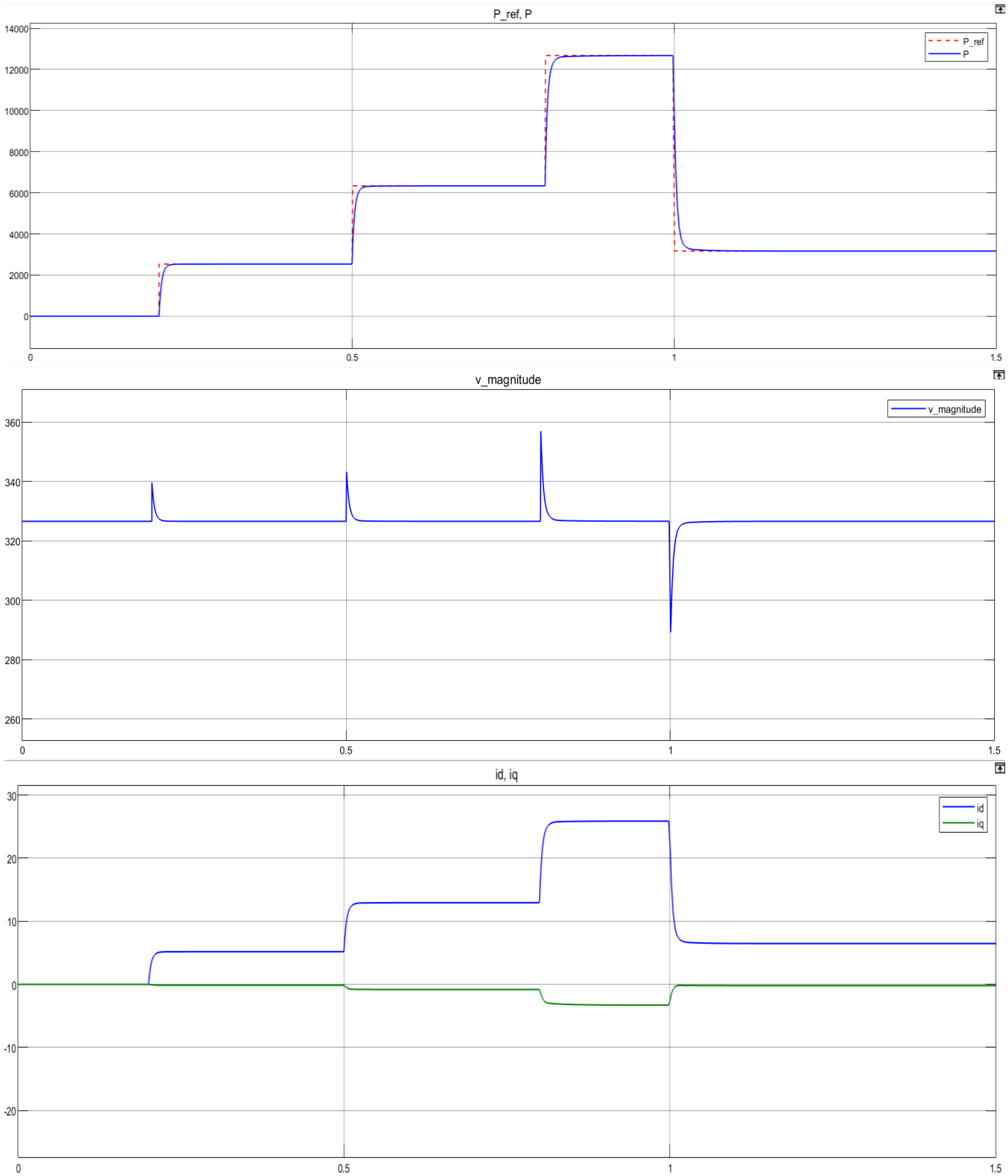

Figure 14 (a) (top) Active-power (blue) tracking under step-sequenced reference power (red). (b) Voltage magnitude. (c) currents id (blue) and iq (green).

4.2 Active-Power Step Response under varying Grid Strengths

This test extends the previous one by evaluating the active-power reference step response under different grid strengths. The reference power follows the same step sequence, while the converter operates under two grid conditions corresponding to weak grid (SCR = 1) and strong grid (SCR = 10).

Figures 15 (a) and (b) illustrate how the calculated active-power tracks the reference in both cases. Under weak grid conditions, the response is slightly slower, whereas in the strong grid, the active-power settles almost instantly after each step. This verifies the behaviour of RFPSC as having faster and better damped response with reduced overshoot and short settling time, compared with the conventional PSC behaviour reported in [28].

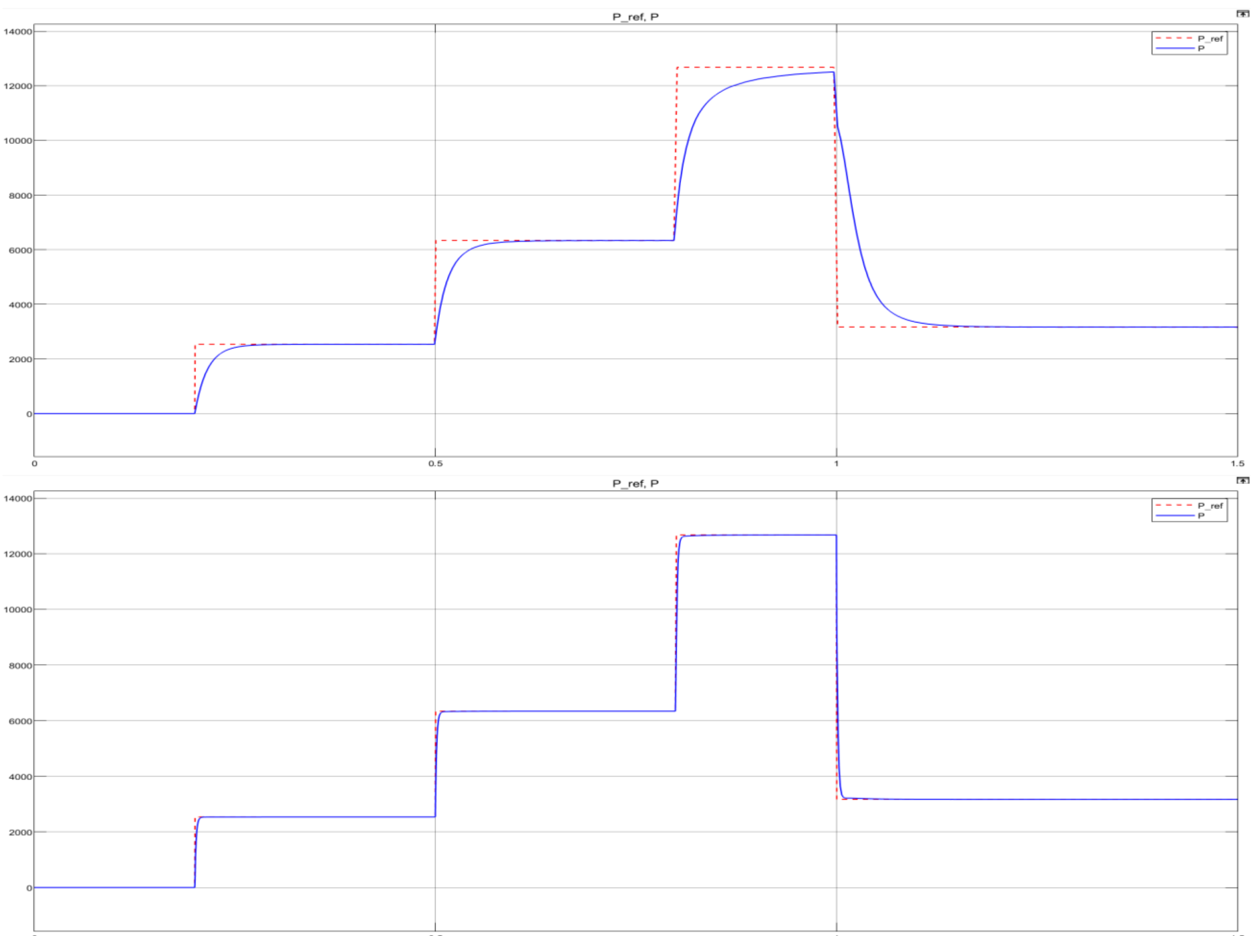

Figure 15 (a) (top) Active-power (blue) tracking under step-sequenced reference power (red) under weak grid conditions (SCR =1). (b) Active-power (blue) tracking under step-sequenced reference power (red) under strong grid conditions (SCR =10).

Figures 15 (c) and (d) demonstrate the corresponding frequency behaviour under the power control law from equation (1), for weak and strong grid conditions respectively. Each reference power step produces a transient deviation in the converter frequency ω_c which then rapidly returns to the grid's fundamental frequency as soon as the power balance is restored. In the weak grids these deviations recover slower, reflecting the slower power-exchange dynamics, whereas in strong grid conditions, they appear as brief spikes. These results confirm that the RFPSC implementation is able to maintain fast synchronization and stable power tracking across grid strengths.

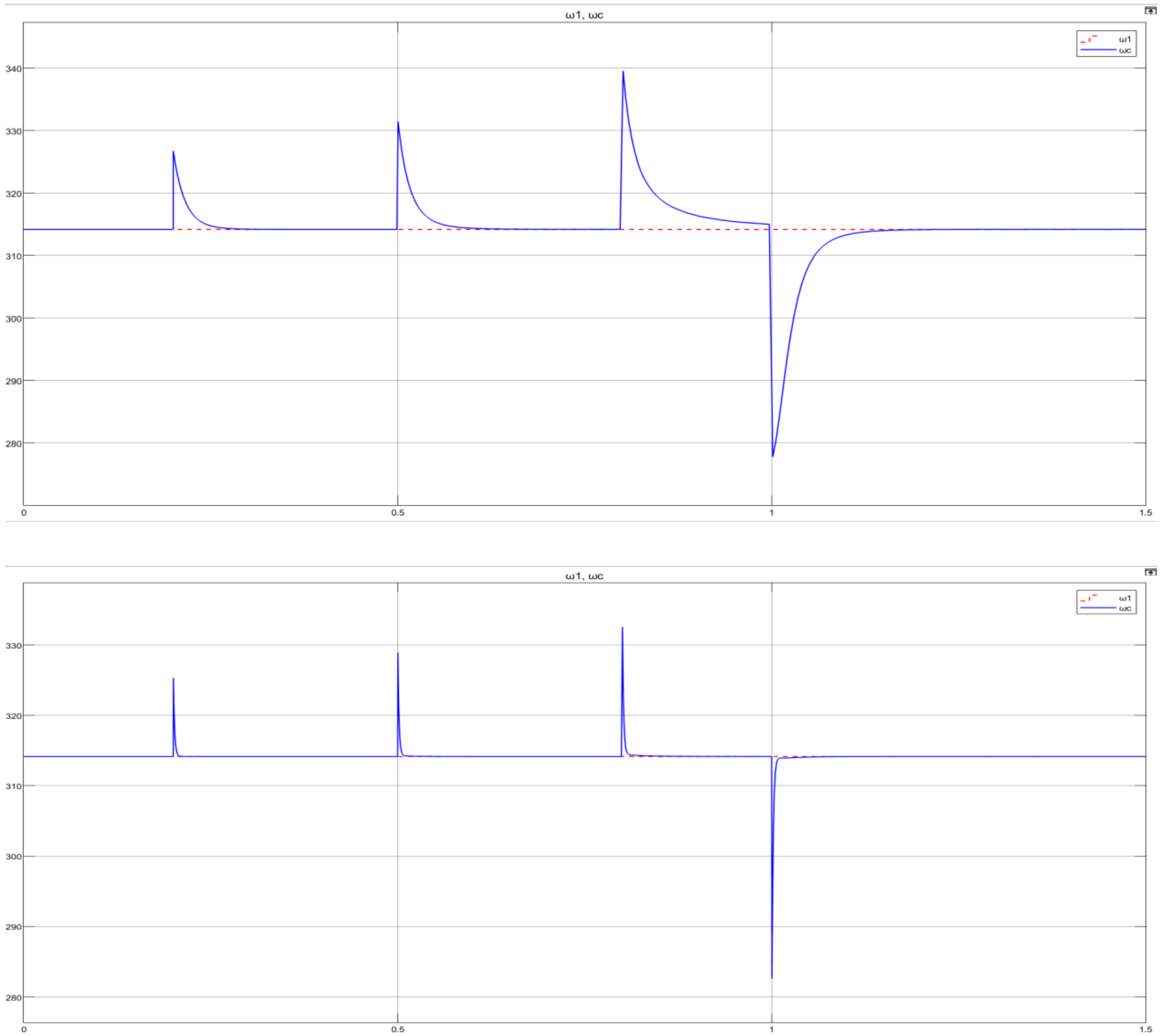

Figure 15 (c) (top) Converter frequency ω_c (blue) response to step-sequenced reference power under weak grid conditions (SCR =1). (d) Converter frequency ω_c (blue) response to step-sequenced reference power under strong grid conditions (SCR =10).

The sharp but non-oscillatory spikes in strong-grid operation further confirm that the converter acts as a damped first-order system, where the frequency deviations follow the power imbalance without introducing resonant behaviour.

4.3 Frequency Deviation Response

To extend the test sequences covered in [28], the frequency deviation test is conducted, as reported in [23]. The grid frequency ω_g is ramped down by 1 Hz and held for a moment before being ramped back up to its nominal value. The grid strength is set at SCR =10, and the P_{ref} is set at 0.25 p.u. Figure 16 (a) shows how the converter frequency ω_c closely follows the grid frequency variation, while Figure 16 (b) illustrates how the active power P changes proportionally with this deviation, following the relation given in [23].

$$P = P_{ref} + \frac{1}{K_p}\left(\omega_1 - \omega_c\right) \qquad (10)$$

These results demonstrate that the RFPSC enhancement retains the inherent power-frequency coupling characteristics of the classical PSC method.

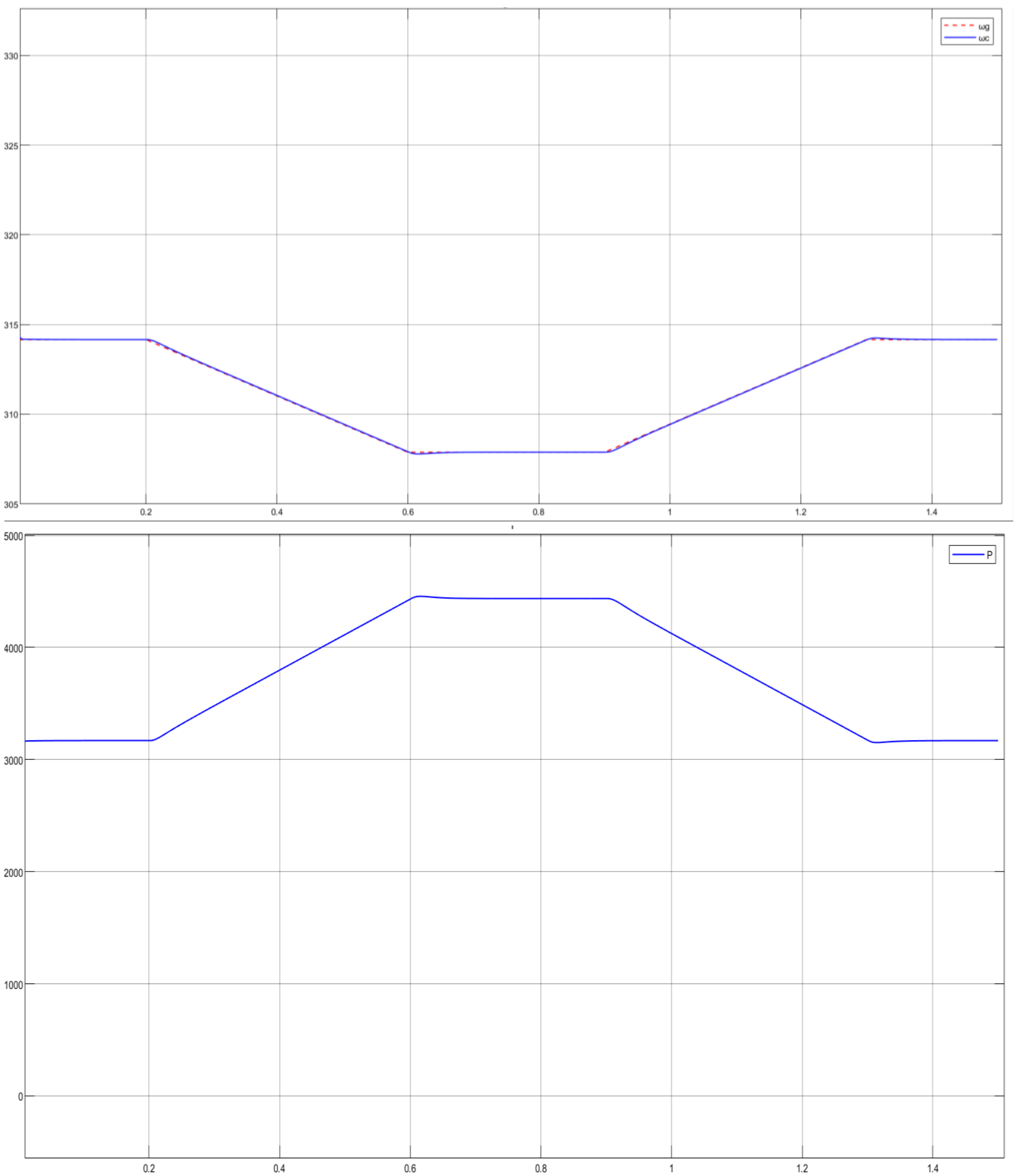

Figure 16 (a) (top) Converter frequency ω_c (blue) tracking grid frequency ω_g (red) during frequency transients. (b) Calculated active-power P variation in response to a -1 Hz grid frequency transient.

5. Summary

In summary, this thesis implemented and validated the RFPSC method in the Simulink environment. The model was implemented as per the design and control structure presented in [28], including the power control law, the reference-feedforward path, the active resistance, and the grid model. The model further retains the analytic gain selection proposed in [23]. The implemented model was evaluated under steady-state, step-response, and frequency deviations scenarios.

The results of the simulation show that the RFPSC implementation achieves the expected improvements over the classical PSC formulation. In steady-state, the converter synchronizes inherently with the grid, with zero active-power reference, confirming correct initialization of the closed-loop structure. The computed active-power was observed to track the reference value effectively. Similarly, the active-power step response tests confirmed that the RFPSC delivered effective tracking across weak, moderate, and strong grids. Under weak grids, the closed loop response stayed stable, but with a slower settling time, while under strong grid, the tracking demonstrated fast rise times with no overshoot. These behaviours align with the RFPSC literature in [28] about the near-perfect pole-zero cancellation inherent to the technique, resulting in a first-order-like system. The results thus verify the analytical claim that the RFPSC performance remains robust irrespective of the SCR ratio.

Moreover, a test involving grid frequency deviations showed that the converter's internal frequency closely tracked the grid's fundamental frequency, indicating the power-frequency coupling inherent to the PSC-based control. The resulting active-power response showed the expected proportional dependence on the frequency deviation.

Overall, the simulation results confirm the successful implementation of the RFPSC technique in the MATLAB and Simulink environment. The findings validate its stable, fast, and robust closed-loop behaviour, supporting its suitability for GFM operation in modern power systems transitioning towards a converter-dominated generation.

Since this thesis adopts the standard assumption of a purely inductive grid, as future work, extending the implementation to include generic grid impedances (including resistive and capacitive components), would broaden the scope of assessment of the controller, and align it with practical networks.

6. References

[1] P. Kundur, *Power System Stability and Control*. New York, NY, USA: McGraw-Hill, 1994.

[2] ENTSO-E, *Inertia and Rate of Change of Frequency (RoCoF)*, Brussels, Belgium, 2020.

[3] C. -C. Chu, S. -H. Lee, K. L. Lian, J. -H. Liu and Y. -J. Lin, "A Survey of Global Revisions to Grid Codes on System Inertia and Frequency Stability in Power Grids with High Renewable Energy Integration," 2025 IEEE Industry Applications Society Annual Meeting (IAS), Taipei, Taiwan, 2025, pp. 1-8, doi: 10.1109/IAS62731.2025.11061388.

[4] S. Li, H. Wang, Y. Huang, G. He, C. Liu and W. Wang, "Dynamic Interaction and Stability Analysis of Grid-following Converter Integrated Into Weak Grid," in CSEE Journal of Power and Energy Systems, vol. 11, no. 2, pp. 552-566, March 2025, doi: 10.17775/CSEEJPES.2024.04920.

[5] L. Zhou, "Risk Assessment of Broadband Oscillation in Hybrid Integration of Multi-Type Grid-Following and Grid-Forming Devices," 2025 4th International Conference on Smart Grids and Energy Systems (SGES), Guizhou, China, 2025, pp. 162-170, doi: 10.1109/SGES66701.2025.11155900.

[6] M. Zhao, H. Wang, M. Zhang, G. He and C. Liu, "Analysis of Broadband Oscillation Suppression Effect of Grid-forming Converter," 2024 4th International Conference on Energy Engineering and Power Systems (EEPS), Hangzhou, China, 2024, pp. 1092-1096, doi: 10.1109/EEPS63402.2024.10804454.

[7] J. Rocabert, A. Luna, F. Blaabjerg, and P. Rodríguez, "Control of power converters in AC microgrids," *IEEE Trans. Power Electron.*, vol. 27, no. 11, pp. 4734–4749, Nov. 2012, doi: 10.1109/TPEL.2012.2199334.

[8] Q. -C. Zhong and G. Weiss, "Synchronverters: Inverters That Mimic Synchronous Generators," in IEEE Transactions on Industrial Electronics, vol. 58, no. 4, pp. 1259-1267, April 2011, doi: 10.1109/TIE.2010.2048839.

[9] S. D'Arco and J. A. Suul, "Virtual synchronous machines — Classification of implementations and analysis of equivalence to droop controllers for microgrids," 2013 IEEE Grenoble Conference, Grenoble, France, 2013, pp. 1-7, doi: 10.1109/PTC.2013.6652456.

[10] R. Rosso, X. Wang, M. Liserre, X. Lu and S. Engelken, "Grid-Forming Converters: Control Approaches, Grid-Synchronization, and Future Trends—A Review," in IEEE Open Journal of Industry Applications, vol. 2, pp. 93-109, 2021, doi: 10.1109/OJIA.2021.3074028.

[11] A. Tarrasó, J. I. Candela, J. Rocabert, Z. Miletic and A. Luna, "Grid Forming Control for Power Converters Based on an Inertial Phase Locked Loop (IPLL)," in IEEE Access, vol. 11, pp. 76008-76019, 2023, doi: 10.1109/ACCESS.2023.3297742.

[12] ENTSO-E, “Grid forming capability of power park modules: First interim report in technical requirements,” Brussels, Belgium: May 2024. [Online]. Available: https://www.entsoe.eu.

[13] P. Kundur et al., "Definition and classification of power system stability IEEE/CIGRE joint task force on stability terms and definitions," in IEEE Transactions on Power Systems, vol. 19, no. 3, pp. 1387-1401, Aug. 2004, doi: 10.1109/TPWRS.2004.825981.

[14] S. D'Arco, J. A. Suul and O. B. Fosso, "Small-signal modelling and parametric sensitivity of a Virtual Synchronous Machine," 2014 Power Systems Computation Conference, Wroclaw, Poland, 2014, pp. 1-9, doi: 10.1109/PSCC.2014.7038410.

[15] K. C. Pradhan and K. B. Mohanty, “Enhancing inertia in parallel VSGs: A power distribution strategy with washout filtering and adaptive virtual impedance,” e-Prime – Advances in Electrical Engineering, Electronics and Energy, vol. 12, 2025, Art. no. 100989, doi: 10.1016/j.prime.2025.100989.

[16] D. Sharma and S. Mishra, "Disturbance-Observer-Based Frequency Regulation Scheme for Low-Inertia Microgrid Systems," in IEEE Systems Journal, vol. 14, no. 1, pp. 782-792, March 2020, doi: 10.1109/JSYST.2019.2901749.

[17] T. Nurminen, R. Mourouvin, M. Hinkkanen and J. Kukkola, "Multifunctional Grid-Forming Converter Control Based on a Disturbance Observer," in IEEE Transactions on Power Electronics, vol. 39, no. 10, pp. 13023-13032, Oct. 2024, doi: 10.1109/TPEL.2024.3433503.

[18] D. Pan, X. Wang, F. Liu and R. Shi, "Transient Stability Analysis of Droop-Controlled Grid-Connected Converters With Inertia Emulating Low-Pass Filters," 2019 IEEE Energy Conversion Congress and Exposition (ECCE), Baltimore, MD, USA, 2019, pp. 34-40, doi: 10.1109/ECCE.2019.8912990.

[19] L. Zhang, L. Harnefors and H. -P. Nee, "Power-Synchronization Control of Grid-Connected Voltage-Source Converters," in IEEE Transactions on Power Systems, vol. 25, no. 2, pp. 809-820, May 2010, doi: 10.1109/TPWRS.2009.2032231.

[20] L. Zhang, L. Harnefors and H. -P. Nee, "Interconnection of Two Very Weak AC Systems by VSC-HVDC Links Using Power-Synchronization Control," in IEEE Transactions on Power Systems, vol. 26, no. 1, pp. 344-355, Feb. 2011, doi: 10.1109/TPWRS.2010.2047875.

[21] L. Zhang, H. -P. Nee and L. Harnefors, "Analysis of Stability Limitations of a VSC-HVDC Link Using Power-Synchronization Control," in IEEE Transactions on Power Systems, vol. 26, no. 3, pp. 1326-1337, Aug. 2011, doi: 10.1109/TPWRS.2010.2085052.

[22] H. Wu and X. Wang, "Design-Oriented Transient Stability Analysis of Grid-Connected Converters With Power Synchronization Control," in IEEE Transactions on Industrial Electronics, vol. 66, no. 8, pp. 6473-6482, Aug. 2019, doi: 10.1109/TIE.2018.2875669.

[23] L. Harnefors, M. Hinkkanen, U. Riaz, F. M. M. Rahman and L. Zhang, "Robust Analytic Design of Power-Synchronization Control," in IEEE Transactions on Industrial Electronics, vol. 66, no. 8, pp. 5810-5819, Aug. 2019, doi: 10.1109/TIE.2018.2874584.

[24] S. E. Sati, A. Al-Durra, H. Zeineldin, T. H. M. El-Fouly, and E. F. El-Saadany, “A novel virtual inertia-based damping stabilizer for frequency control enhancement for islanded microgrid,” Int. J. Electr. Power Energy Syst., vol. 155, pt. B, 2024, Art. no. 109580, doi: 10.1016/j.ijepes.2023.109580.

[25]J. K. M. Becker, A. M. Kettner, L. Reyes-Chamorro, Z. Zou, M. Liserre and M. Paolone, "Harmonic Power-Flow Study of Polyphase Grids With Converter-Interfaced Distributed Energy Resources—Part II: Model Library and Validation," in IEEE Transactions on Smart Grid, vol. 13, no. 1, pp. 470-481, Jan. 2022, doi: 10.1109/TSG.2021.3120081.

[26] C. Kasnakoğlu and A. Cakiroglu, “Modeling of grid forming inverters and analysis under different control approaches,” Thesis, 2024, doi: 10.13140/RG.2.2.15358.09285.

[27] V. Steinsland, L. M. Kristensen, and S. Zhang, “Modelling and validation of power electronics converter systems using coloured Petri nets,” arXiv, arXiv:2212.06781, Dec. 2022. [Online]. Available: https://arxiv.org/abs/2212.06781.

[28] L. Harnefors, F. M. M. Rahman, M. Hinkkanen and M. Routimo, "Reference-Feedforward Power-Synchronization Control," in IEEE Transactions on Power Electronics, vol. 35, no. 9, pp. 8878-8881, Sept. 2020, doi: 10.1109/TPEL.2020.2970991.

[29] A. M. Saleh, I. Vokony, M. A. Khan, M. Waseem, and A. N. A. Ahmed, “Power system stability in the era of energy transition: Importance, opportunities, challenges, and future directions,” Energy Convers. Manag.: X, vol. 24, 2024, Art. no. 100820, doi: 10.1016/j.ecmx.2024.100820.